Low-power plasmon–soliton in realistic nonlinear planar structures

Wiktor Walasik,[1,2] Virginie Nazabal,[3] Mathieu Chauvet,[4] Yaroslav Kartashov,[5] and Gilles Renversez[1,*]

[1]*Université d´Aix-Marseille, CNRS, Institut Fresnel UMR 7249, Campus de St. Jérôme, Marseille 13013, France*

[2]*ICFO—Institut de Ciències Fotòniques, Universitat Politècnica de Catalunya, Castelldefels, Barcelona 08860, Spain*

[3]*Sciences Chimiques de Rennes, CNRS, UMR 6226, Université de Rennes I, Campus de Beaulieu, Rennes 35042, France*

[4]*FEMTO-ST, CNRS, UMR 6174, Université de Franche-Comté, 16 Route de Gray, Besançon 25000, France*

[5]*Institute of Spectroscopy, Russian Academy of Sciences, Troitsk, Moscow Region 142190, Russia*

**Corresponding author: gilles.renversez@fresnel.fr*

Received May 17, 2012; revised August 30, 2012; accepted September 17, 2012;
posted September 26, 2012 (Doc. ID 168477); published November 6, 2012

We study the propagation of nonlinear waves in layered nonlinear dielectric/linear dielectric/metal planar structures. We develop vector models that describe the light propagation in such configurations and allow us to obtain both one- and two-dimensional solutions. We compute the nonlinear dispersion relation and the field profiles, and estimate losses. We use our models to design realistic structures, in terms of linear and nonlinear properties, which support soliton waves with a plasmon tail at low peak power around or below 1 GW/cm^2. These results open the way for potential observation of such states in chalcogenide waveguides associated with silica and metal films. In the proposed structures, the nonlinearity confines the field in both transverse directions. A recordable plasmonic part of the field extends in air.

OCIS codes: 190.6135, 240.6680, 230.7400, 190.3270.

It is now well established that plasmonics is a flourishing research field that attracts a lot of attention [1]. Similarly, optical solitons have been studied for more than 40 years and are still an active research domain [2,3]. Several works have been recently published about self-sustained solutions that combine soliton and plasmon features in metal/nonlinear dielectric structures [4–6]. The first descriptions of one-dimensional (1D) nonlinear plasmon–soliton and surface waves on metal/dielectric and dielectric/dielectric interfaces were given more than 30 years ago [7–11]. The plasmon–soliton state consists of a spatial soliton coupled with a plasmon, though different terms were used to describe such states (see. Fig. 2 in [9]).

Nevertheless, up to now no experimental results have been published on the issue of plasmon–soliton coupling. The main reason is that for the proposed structures the nonlinear refractive index change required for the formation of plasmon–soliton waves is too high compared to the one attainable in real materials, or equivalently the peak power is too high using values of nonlinear coefficients of conventional materials used in integrated optics [2,12].

In this Letter, we describe for the first time planar structures made of conventional materials supporting low-peak-power solutions that combine a two-dimensional (2D) soliton profile with a plasmonic field. They are composed of a chalcogenide glass coated with silica and gold films. It is worth mentioning that structures similar to the ones we propose have already been fabricated [13] even they were not intended for plasmon–soliton studies. Moreover, optical solitons have already been observed in chalcogenide planar waveguides for peak power around 2 GW/cm^2 [14].

The configurations we propose offer the possibility to realize an experiment where the soliton–plasmon wave can be easily excited using low-peak-intensity beams [14], and where the plasmonic part of the nonlinear solution can be recorded using near-field optics because it is strong enough at the interface between the metal layer and the external dielectric. Furthermore, this kind of configuration can be made suitable for sensor applications since the decaying part of the plasmon field can be located at a metal/air or at a metal/water interface.

We found out that to couple in the same wave a pronounced low-power soliton with a plasmon part that extends in a linear low-index external medium, a nonlinear dielectric/linear dielectric/metal structure is needed. To describe such a structure, a four-layer model is necessary (see Fig. 1). Due to the plasmon part of the nonlinear waves, a vector approach is required. Therefore, we expand the 1D vector model used for a symmetric three-layer configuration made of a metal film embedded in semi-infinite nonlinear dielectric regions [9] to study the propagation of nonlinear waves in a four-layer configuration. A complete study of the solutions in such structures will be published elsewhere. We find that no TM-like nonlinear waves with or without a pronounced soliton part can be obtained if the metal layer is replaced by a dielectric even at powers up to five times above the material damage threshold.

In our method, the nonlinear solution of a 1D problem obtained in the four-layer configuration is used to construct the 2D nonlinear profile, which is not the case in [4,5].

Let us consider the propagation of nonlinear light waves in a layered metal/nonlinear dielectric/linear

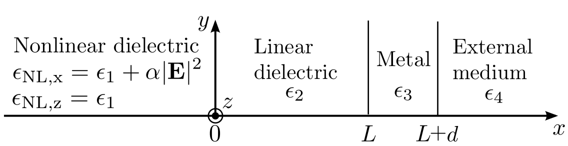

Fig. 1. Geometry of the four-layer nonlinear model used to study three-layer structures. ϵ_j denotes the linear permittivity of the jth layer ($j \in \{1, 2, 3, 4\}$).

dielectric structure presented in Fig. 1. We consider a Kerr type nonlinearity of the form $\alpha(x) = \mathcal{H}(-x)\epsilon_0 c\epsilon(x)n_2$, where $\mathcal{H}(x)$ denotes the Heaviside step function, ϵ_0 the vacuum permittivity, c the speed of light, n_2 the Kerr nonlinear coefficient, and $\epsilon(x)$ the stepwise linear permittivity profile as defined in Fig. 1. For TM-polarized light the electromagnetic field is written as $\mathbf{E} = [E_x, 0, E_z]$ and $\mathbf{H} = [0, H_y, 0]$. For the 1D problem we look for stationary solutions in the following form:

$$\mathbf{E}(x,z,t) = \mathbf{E}_{\mathrm{NL}}(x)\exp[i(\beta_{\mathrm{NL}}k_0 z - \omega t)], \tag{1}$$

where $k_0 = 2\pi/\lambda$, λ denotes the free-space wavelength and β_{NL} is the effective index of this nonlinear wave. The magnetic field $\mathbf{H}$ has the same form.

First we find the x-component of the $\mathbf{E}_{\mathrm{NL}}$ field denoted by $E_{\mathrm{NL},x}(x)$ by solving the 1D nonlinear problem along x direction. As in [9], we assume that $|E_z| \ll |E_x|$ and we expand the nonlinear term in the wave equation into Taylor series with respect to the small parameter $\alpha|E_{\mathrm{NL},x}|^2$. This results in a nonlinear wave equation:

$$\frac{d^2E_{\mathrm{NL},x}}{dx^2} - k_0^2 q^2(x)E_{\mathrm{NL},x} + k_0^2 a(x)E_{\mathrm{NL},x}^3 = 0, \tag{2}$$

in which $a(x) = \beta_{\mathrm{NL}}^2\alpha(x)/\epsilon(x)$ and $q^2(x) = \beta_{\mathrm{NL}}^2 - \epsilon(x)$. The solution of Eq. (2) provides analytical expressions for $E_{\mathrm{NL},x}(x)$, and Maxwell's equations yield the expressions for the remaining [$E_{\mathrm{NL},z}(x)$ and $H_{\mathrm{NL},y}(x)$] field components. Finally using the field continuity conditions at the interfaces, we get the analytical implicit form of the nonlinear dispersion relation of the four-layer model:

$$\Phi_+(\tilde{q}_4 + \tilde{q}_3)\exp(2k_0\tilde{q}_3\epsilon_3 d) + \Phi_-(\tilde{q}_4 - \tilde{q}_3) = 0, \tag{3}$$

$$\Phi_\pm = \left(1 \pm \frac{\tilde{q}_{1\mathrm{NL}}}{\tilde{q}_3}\right) + \left(\frac{\tilde{q}_{1\mathrm{NL}}}{\tilde{q}_2} \pm \frac{\tilde{q}_2}{\tilde{q}_4}\right)\tanh(k_0\tilde{q}_2\epsilon_2 L), \tag{4}$$

where $\tilde{q}_j = q(x)/\epsilon(x)$ in the jth layer, $\tilde{q}_{1\mathrm{NL}} = \tilde{q}_1\tanh(k_0\tilde{q}_1\epsilon_1 x_0)$, and x_0 denotes the center of the soliton part of the nonlinear wave that appears in the expression for the field in the nonlinear dielectric layer: $E_{\mathrm{NL},x}(x) = [2/a(x)]^{1/2}\tilde{q}_1\epsilon_1\,\mathrm{sech}[k_0\tilde{q}_1\epsilon_1(x - x_0)]$. From Eq. (3), we compute the allowed β_{NL} values of this nonlinear 1D problem that are then used to determine all the field components from Eq. (2). In Fig. 2, the dispersion relation obtained by solving Eq. (3) (dashed line) is presented. The 1D intensity profile for a peak power around 1 $\mathrm{GW/cm^2}$ is shown in Fig. 3. We verify *a posteriori* that the assumption $|E_z| \ll |E_x|$ is fulfilled in the nonlinear medium (in our example $|E_x|/|E_z| > 50$ for soliton peak intensities <10 $\mathrm{GW/cm^2}$). From the limit case $L \to 0$ in Eqs. (3) and (4), we can recover the results obtained in [9].

Knowing the x-profiles of the electric field $\mathbf{E}_{\mathrm{NL}}(x)$ for the 1D nonlinear problem, we look for solutions that are also localized along y-axis using the 2D model. In this approach, we assume the same arrangement of materials along x-axis and suppose that they are infinite along y-axis. We consequently look for solutions of the form

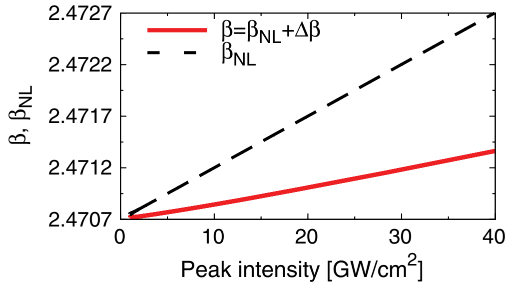

Fig. 2. (Color online) Dispersion curves obtained from the 1D model (dashed line) and from the 2D model (solid line). Parameters used are $\epsilon_1 = 2.4707^2$, $n_2 = 10^{-13}$ $\mathrm{cm^2/W}$ (chalcogenide glass), $\epsilon_2 = 1.443^2$ (silica), $\epsilon_3 = -96$ (gold), $\epsilon_4 = 1$ (air), $L = 15$ nm, $d = 40$ nm, $\lambda = 1.55$ μm.

$$\mathbf{E}(x,y,z,t) = \mathbf{E}_{\mathrm{NL}}(x)\psi(y,z)\exp[i(\beta_{\mathrm{NL}}k_0 z - \omega t)]. \tag{5}$$

To simplify the equation $\nabla\times(\nabla\times\mathbf{E}) - \epsilon k_0^2\mathbf{E} = 0$ we search again for TM modes imposing the relation $(\partial_x(\epsilon_x E_x) = -\partial_z(\epsilon_z E_z))$. This approximation allows us to obtain a differential equation for E_x. Finally, multiplying this differential equation by $E_{\mathrm{NL},x}$ and assuming that $\psi(y,z) = \psi(y)\exp(i\Delta\beta k_0 z)$, we integrate over the x-direction to get a nonlinear second-order differential equation for $\psi(y)$ [4,5]:

$$\left[F - (\beta_{\mathrm{NL}} + \Delta\beta)^2 - G + \frac{1}{k_0^2}\frac{d^2\cdot}{dy^2} + A|\psi|^2\right]\psi = 0, \tag{6}$$

in which the parameters are

$$G = \langle\epsilon(x)E_{\mathrm{NL},x}^2\rangle,\ F = \frac{1}{k_0^2}\left\langle\frac{d^2E_{\mathrm{NL},x}}{dx^2}E_{\mathrm{NL},x}\right\rangle,$$
$$A = \left\langle\frac{3\alpha(x)}{\epsilon(x)k_0^2}E_{\mathrm{NL},x}\left[E_{\mathrm{NL},x}\frac{d^2E_{\mathrm{NL},x}}{dx^2} + 2\left(\frac{dE_{\mathrm{NL},x}}{dx}\right)^2\right]\right.$$
$$\left. + \alpha(x)E_{\mathrm{NL},x}^4\right\rangle,\ \text{and}\ \langle\bullet\rangle = \int_{-\infty}^{+\infty}\bullet\,\mathrm{d}x\Big/\int_{-\infty}^{+\infty}E_{\mathrm{NL},x}^2\mathrm{d}x. \tag{7}$$

It is worth mentioning that the last term in A is the leading one. We must emphasize that the used nonlinear separation of variables is a crude approximation in our case since the field widths along x and y are comparable. Nevertheless, the comparison of the normalized power of the obtained solution with the one of the Townes soliton reveals the difference of about 20%, which indicates on reasonable accuracy of this approach. A more

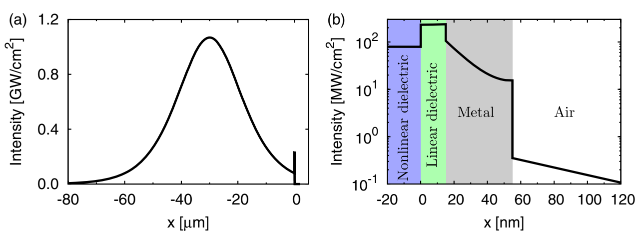

Fig. 3. (Color online) Intensity profiles for low-power solutions of 1D problem. (a) Full solution and (b) zoom on the plasmon part at the metal interfaces. Material and geometric parameters are the same as in Fig. 2, $x_0 = -30$ μm.

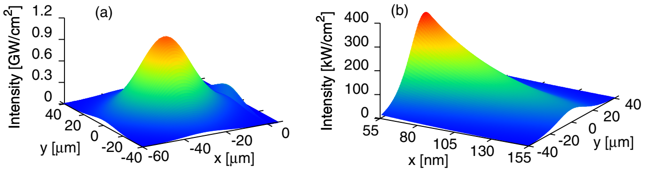

Fig. 4. (Color online) 2D intensity profile for the low-power plasmon–soliton in the four-layer planar nonlinear configuration. (a) Full solution and (b) zoom of the plasmon part at the metal/air interface. Parameters same as in Fig. 3.

rigorous approach requires the development of a truly 2D model.

In our 2D model, the peak power is set to the value previously obtained from the 1D model, in order to preserve the properties of the 1D nonlinear solution since the superposition principle is no longer valid [15]. Using the test function $\psi(y) = \mathrm{sech}(y/\omega_y)$ to solve Eq. (6), we find the necessary values of parameters $\omega_y = [2/(k_0^2 A)]^{1/2}$ and $\Delta\beta$. The solid line in Fig. 2 shows the power dependency of the effective index β of the 2D plasmon–soliton:

$$\beta = \beta_{\mathrm{NL}} + \Delta\beta = [G + F + (k_0\omega_y)^{-2}]^{1/2}. \qquad (8)$$

In Fig. 4 we present an example of such 2D plasmon–soliton profiles. The peak intensity is found to be $1.07\ \mathrm{GW/cm^2}$ (which is twice lower than intensities required for formations of solitons in chalcogenide waveguides [14]). The resulting value of the effective index is $\beta = 2.470717$, while half-widths along x and y directions are given by $\omega_x \approx 15.2$ μm and $\omega_y \approx 18.4$ μm. It is important to note that in the proposed structure the low-intensity solution exists even if we use the nonlinear Kerr coefficient of chalcogenide glass $n_2 = 10^{-13}\ \mathrm{cm^2/W}$ [12], which is much lower than the ones used in previous works on plasmon–solitons [4,5,9]. Three-layer structures made of the same materials as those considered here can also be designed to support low peak power ($\approx 0.6\ \mathrm{GW/cm^2}$) plasmon–solitons at a metal/water interface.

The propagation losses in the structure are estimated using the method based on the field profiles and imaginary parts of the permittivities described in [9], which is similar to the one from [5]. For the examples shown in Figs. 3 and 4 (assuming $\Im m(\epsilon_1) = \Im m(\epsilon_2) = 10^{-5}$, $\Im m(\epsilon_3) = 10$), the losses are at the level $\Im m(\beta) \approx 0.8 \times 10^{-5}$, corresponding approximately to 2.8 dB/cm. Even though the part of electromagnetic energy located in the metal layer is small compared to the total one (less than 2×10^{-3}%) and the level of losses is small, a more rigorous approach should take into account the imaginary parts of the permittivities and of the propagation constant at the first step of the calculus. The plasmon peak light intensity is one-tenth of the soliton one that corresponds to a peak electric field value in the metal layer of approximatively 4.5×10^6 V/m which makes it recordable using current near-field optics techniques [1].

Our simple planar structure can be improved or tuned by using metal gratings or nanoparticles at the surface of the metal layer [1]. In accordance with the Vakhitov–Kolokolov stability criterion, monotonic growth of power with increase of propagation constant indicates the stability of the obtained soliton family. The required complete study of the stability of the found stationary solutions [using finite-difference time-domain (FDTD), for example] will be provided elsewhere. Furthermore, we can mention that we are not looking for propagation as long as in fiber optics, and that losses will have to be taken into account in the study of stability.

In conclusion, we have described a simple planar structure made of conventional materials that support a soliton with a plasmonic part on the tail having low peak powers, comparable to powers of solitons in chalcogenide waveguides [14]. The structure we propose is a first step toward the experimental demonstration of a plasmonic sensor involving plasmon–soliton coupling. Experimental work is in progress to validate our modeling results.

This work was supported by the European Commission through the Erasmus Mundus Joint Doctorate Programme Europhotonics (Grant No. 159224-1-2009-1-FR-ERA MUNDUS-EMJD) and by the PICS CNRS program CAPLA.

References

1. S. A. Maier, *Plasmonics: Fundamentals and Applications* (Springer, 2007).
2. Y. S. Kivshar and G. P. Agrawal, *Optical Solitons, From Fibers to Photonic Crystals* (Academic, 2003).
3. F. Drouart, G. Renversez, A. Nicolet, and C. Geuzaine, J. Opt. A: Pure Appl. Opt. **10**, 125101 (2008).
4. E. Feigenbaum and M. Orenstein, Opt. Lett. **32**, 674 (2007).
5. A. R. Davoyan, I. V. Shadrivov, and Y. S. Kivshar, Opt. Express **17**, 21732 (2009).
6. K. Y. Bliokh, Y. P. Bliokh, and A. Ferrando, Phys. Rev. A **79**, 41803 (2009).
7. V. M. Agranovich, V. S. Babichenko, and V. Y. Chernyak, JETP Lett. **32**, 512 (1980).
8. W. J. Tomlinson, Opt. Lett. **5**, 323 (1980).
9. J. Ariyasu, C. T. Seaton, G. I. Stegeman, A. A. Maradudin, and R. F. Wallis, J. Appl. Phys. **58**, 2460 (1985).
10. N. N. Akhmediev, Sov. Phys. JETP **56**, 299 (1982).
11. A. A. Maradudin, in *Optical and Acoustics Waves in Solids —Modern Topics*, M. Borissov, ed. (World Scientific, 1983), pp. 72–142.
12. G. Boudebs, F. Sanchez, J. Troles, and F. Smektala, Opt. Commun. **199**, 425 (2001).
13. V. Nazabal, F. Charpentier, J.-L. Adam, P. Nemec, H. Lhermite, M.-L. Brandily-Anne, J. Charrier, J.-P. Guin, and A. Moreac, Int. J. Appl. Ceram. Technol. **8**, 990 (2011).
14. M. Chauvet, G. Fanjoux, K. P. Huy, V. Nazabal, F. Charpentier, T. Billeton, G. Boudebs, M. Cathelinaud, and S.-P. Gorza, Opt. Lett. **34**, 1804 (2009).
15. R. A. Sammut, C. Pask, and Q. Y. Li, J. Opt. Soc. Am. B **10**, 485 (1993).